Aluminosilicate Mesoporous Molecular Sieve MCM-48

Antonio A. Romero,[†] María D. Alba,[‡] and Jacek Klinowski*

Department of Chemistry, University of Cambridge, Lensfield Road, Cambridge CB2 1EW, U.K.

Received: April 30, 1997; In Final Form: September 19, 1997[⊗]

Mesoporous aluminosilicate molecular sieves with the MCM-48 structure and atomic Si/Al ratios of 15−40 have been synthesized using aluminum chloride hexahydrate and aluminum sulfate as the sources of aluminum. The products were characterized by powder X-ray diffraction (XRD), thermal analysis (TG/DTA), diffuse reflectance Fourier-transform infrared (DRIFT), ^{29}Si and ^{27}Al magic-angle-spinning (MAS) NMR, and nitrogen sorption. The quality of the product rapidly deteriorates as the aluminum content of the solid increases. The walls of the mesopores are essentially amorphous, and the local atomic arrangement is similar to that in amorphous aluminosilicates. The regular arrangement of uniform channels is the only element of order. ^{27}Al MAS NMR shows that when aluminum sulfate is used, both 4- and 6-coordinate aluminum is present in the calcined products. On the other hand, when aluminum chloride hexahydrate is used, aluminosilicate MCM-48 can be prepared with all aluminum in 4-coordination and the Si/Al ratio as low as 15. XRD shows that the substitution of the silicon by the larger aluminum atoms leads to a *contraction* of the unit cell.

Introduction

The preparation of the M41S family of mesoporous silicate molecular sieves[1,2] has opened new possibilities in many areas of chemistry and materials science. Progress in the synthesis, characterization, and application of these materials and their transition metal oxide analogues have been reviewed.[3−7] The mesoporous molecular sieves are found to form three distinct phases: a hexagonal phase referred to as MCM-41, a cubic phase (space group *Ia*3*d*) known as MCM-48, and an unstable lamellar phase (MCM-50). Most research has concentrated on MCM-41, and only a few publications dealing with MCM-48 have appeared.[3,8−16]

Given the absence of acid sites and ion-exchange capacity, the purely siliceous MCM-48 is of limited use as a catalyst. Much attention has therefore been devoted to isomorphous substitution of Al[10,13] as well as Mn, V, Cr, and Ti,[10,12,15,16] in the silicate network. We describe the synthesis and characterization of aluminosilicate MCM-48 with Si/Al = 15−40 using aluminum chloride hexahydrate and aluminum sulfate as the sources of aluminum. We have approached the synthesis of aluminosilicate MCM-48 materials in the same way as that used for aluminosilicate MCM-41, thus allowing us to compare their properties directly. Aware that the atomic arrangement in these materials is essentially amorphous, we shall refer to "crystallinity" in the sense of the regular arrangement of uniform channels, the only element of order. All references to a unit cell, etc., should be interpreted accordingly.

* To whom correspondence should be addressed: Dr. J. Klinowski Department of Chemistry, University of Cambridge, Lensfield Road, Cambridge CB2 1EW, U.K. Telephone: +(44)-1223-33 65 14. FAX: +(44)-1223-33 63 62. E-mail: jk18@cam.ac.uk.

† On leave from Departamento de Química Organica, Universidad de Córdoba, San Alverto Magno s/n, 14004 Córdoba, Spain.

‡ On leave from Departamento de Química Inorganica, Instituto Ciencia de los Materiales, Universidad de Sevilla, C.S.I.C., P.O. Box 874, 41012 Sevilla, Spain.

⊗ Abstract published in *Advance ACS Abstracts,* December 1, 1997.

Experimental Section

Synthesis. The source of silica was tetraethyl orthosilicate (TEOS) and the surfactant was cetyltrimethylammonium bromide (CTAB), both from Aldrich. A solution of cetyltrimethylammonium hydroxide was prepared by batch exchange of a 25 wt % aqueous $C_{16}H_{33}(CH_3)_3NBr$ solution with the IRA-420-(OH) ion-exchange resin (Aldrich). The degree of exchange of the hydroxide for bromide ion was 30%. The sources of aluminum were aluminum chloride hexahydrate (Aldrich) and aluminum sulfate (Fluka-Garantie).

TEOS was added slowly under stirring to a solution of CTAB/OH in a surfactant/silica molar ratio of 1.2. The gel was then stirred for 10 min at room temperature (solution A). A required amount of the desired source of aluminum was dissolved or dispersed in a 0.8 M aqueous solution of KOH (Fisons, A. R. grade). The aluminum solution was added slowly under stirring to solution A. The resulting mixture was stirred for 60 min at room temperature. The reaction mixture was transferred into a Teflon bottle and placed in a furnace at 110 °C. The ethanol produced in the hydrolysis of the TEOS was allowed to evaporate. Aluminosilicate MCM-48 was obtained when part of the water was removed from the gel mixture, so that the mixture became more concentrated in the course of the reaction.[17] MCM-41 was obtained when water was prevented from evaporating from the gel mixture. Table 1 shows the molar and elemental composition of the final gel mixtures (in terms of the Si/Al ratio), the composition of aluminosilicate MCM-48 and MCM-41 (by EDX, see below), and the reaction time. The solid products were recovered by filtration, washed with distilled water, dried in air at 75 °C overnight, and then calcined at 550 °C at a heating rate of 10 °C/min, starting at 200 °C, for 24 h in air. Purely siliceous MCM-48 (sample Si−MCM-48) was made by mixing 7.2 mL of TEOS with 50 mL of CTAB/OH solution under stirring. The gel was treated as described above.

The designation of each sample is composed of two segments separated by a hyphen. The first segment gives the aluminum

S1089-5647(97)01469-7 CCC: $15.00
Published on Web 01/01/1998

TABLE 1: Composition of the Final Gel Mixture and the M41S Products for Different Reaction Times at 110 °C

sample	molar composition final gel mixture	gel Si/Al ratio	sample Si/Al ratio (by EDX)	reaction time (h)
Si−MCM-48	SiO_2:1.2 CTAB/OH			48
AlC48-40	SiO_2:1.2 CTAB/OH:0.09 K_2O:13 H_2O:0.013 Al_2O_3	40	40	12
AlC48-30	SiO_2:1.2 CTAB/OH:0.09 K_2O:13 H_2O:0.017 Al_2O_3	30	33	36
AlS48-20	SiO_2:1.2 CTAB/OH:0.09 K_2O:13 H_2O:0.025 Al_2O_3	20	24	48
AlC48-15	SiO_2:1.2 CTAB/OH:0.32 K_2O:13 H_2O:0.034 Al_2O_3	15	15	60
AlC41-40	SiO_2:1.2 CTAB/OH:0.09 K_2O:13 H_2O:0.013 Al_2O_3	40	45	24
AlC41-30	SiO_2:1.2 CTAB/OH:0.09 K_2O:13 H_2O:0.017 Al_2O_3	30	28	24
AlS41-20	SiO_2:1.2 CTAB/OH:0.09 K_2O:13 H_2O:0.025 Al_2O_3	20	23	48
AlC41-15	SiO_2:1.2 CTAB/OH:0.32 K_2O:13 H_2O:0.034 Al_2O_3	15	15	48

source (AlC for the aluminum chloride hexahydrate and AlS for aluminum sulfate) and the type of aluminosilicate product (48 for MCM-48 and 41 for MCM-41); the second segment gives the Si/Al ratio of the gel mixture. Thus AlC48-40 signifies an aluminosilicate MCM-48 made using aluminum chloride hexahydrate as the source of aluminum from a gel mixture with Si/Al = 40.

Sample Characterization. *Elemental Analysis.* Elemental composition of the calcined samples was determined using a JEOL 5800 scanning electron microscope (SEM) with energy-dispersive X-ray analysis (EDX) at 20 kV. Small fragments of a sample were mounted on carbon tape stuck to a conducting Bakelite mount and scanned with a small raster scan at low magnification (about 100×) in order to cover a representative area of each sample (ca. 1.3 mm^2). The Si/Al molar ratios of calcined MCM-48 and MCM-41 are in close agreement with the composition of the gel mixtures (Table 1), showing that aluminum and silicon from the gel are incorporated into the solid in equal proportions.

Powder X-ray Diffraction (XRD). XRD patterns were recorded using a Philips 1710 powder diffractometer with Cu Kα radiation (40 kV, 40 mA), a step size of 0.02° and a counting time per step of 1 s.

Thermogravimetric and Differential Thermal Analysis. Thermal analysis was performed by simultaneous TG-DTA measurements in flowing nitrogen using the SETARAM thermobalance TG-DTA 92. Samples were heated in the temperature range 20−1000 °C at a heating rate of 8 °C/min.

Diffuse Reflectance Fourier-Transform (DRIFT). DRIFT spectra were recorded on a Bomem MB-100 instrument equipped with an environmental chamber (Spectra Tech, P/N 0030-100) placed in the diffuse reflectance attachment (Spectra Tech, Collector). A resolution of 8 cm^{-1} was used, and 256 scans were averaged to obtain spectra in the 4000−400 cm^{-1} range. Single-beam spectra were measured against KBr reference spectra. The temperature was measured by inserting a thermocouple directly into the sample. Calcined samples were dried at 150 °C for 48 h, diluted to 10 wt % in KBr, and placed in an environmental chamber cell with a 50 mL min^{-1} flow of dehydrated deoxygenated nitrogen, heated to 300 °C and maintained at this temperature for 1 h prior to measuring the spectrum.

Magic-Angle-Spinning (MAS) NMR. MAS NMR spectra were recorded at 9.4 T using a Chemagnetics CMX-400 spectrometer with zirconia MAS rotors 4 mm in diameter spun in air at 8 kHz (for ^{27}Al) and 7.5 mm rotors spun at 3.5 kHz (for ^{29}Si). ^{29}Si MAS NMR spectra were acquired at 79.4 MHz with 90° radiofrequency pulses and 600 s recycle delays. $^{1}H-^{29}Si$ cross-polarization (CP) MAS spectra were recorded with a single-contact pulse sequence with 8 ms contact time, 11.5 μs ^{1}H 90° pulse, 4 s recycle time, and 700 scans. The Hartmann−Hahn condition was established using a sample of kaolinite and the chemical shifts are given in ppm from external tetramethylsilane (TMS). ^{27}Al spectra were measured at 104.3 MHz with <10° pulses and 0.3 s recycle delays. External $Al(H_2O)_6^{3+}$ was used as a reference.

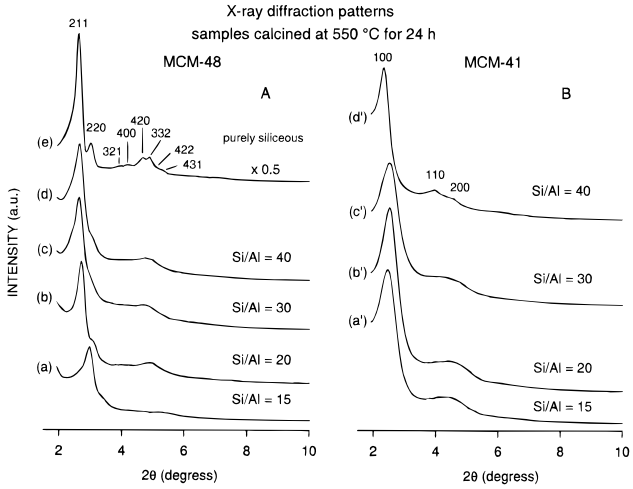

Figure 1. A: XRD patterns of (curve a) AlC48-15, (curve b) AlS48-20, (curve c) AlC48-30, (curve d) AlC48-40, and (curve e) Si−MCM-48. B: XRD patterns of (curve a′) AlC41-15, (curve b′) AlS41-20, (curve c′) AlC41-30, and (curve d′) AlC41-40.

Nitrogen Sorption. Nitrogen adsorption/desorption isotherms were measured at 77 K with a Micrometrics ASAP 2000 instrument. The samples were first outgassed at 250 °C for 24 h. The volume of adsorbed N_2 was normalized to standard temperature and pressure. The BET surface area was calculated with the cross-sectional area of a nitrogen molecule taken as 16.2 $Å^2$ by applying the BET equation for relative pressure between 0.05 and 0.22. *t*-plots were drawn to evaluate the microporosity by comparing the shape of a given isotherm with that of a standard for a nonporous solid selected following the IUPAC recommendation.[18] The pore size distribution (PSD) was calculated using the adsorption branch of the N_2 adsorption/desorption isotherm and the Barrett−Joyner−Halenda (BJH) formula.[19] The cumulative pore volume V_{BJH} of the mesopores was obtained from the PSD curve.

Results and Discussion

XRD. The X-ray power diffraction patterns of calcined samples of aluminosilicate MCM-48 and MCM-41 with different Si/Al ratios (Figure 1) correspond to those of the cubic and hexagonal M41S phases, respectively.[1,2] The peaks are shifted to higher 2θ angles and their intensities are increased in comparison with the as-synthesized samples (patterns not shown). Similar trends were found for aluminosilicate MCM-41,[20−22] where calcination leads to a contraction of unit cell accompanied by the condensation of Si−OH groups monitored by ^{29}Si MAS NMR.

TABLE 2: Cubic Unit Cell Parameter Calculated as $a = d_{211}\sqrt{6}$ of Purely Siliceous and Aluminosilicate MCM-48 Samples and Hexagonal Unit Cell Parameters Calculated as $a = 2d_{100}/\sqrt{3}$ of Aluminosilicate MCM-41 Samples[a]

	unit cell parameter (Å)		
sample	as-synthesized	calcined	contraction
Si−MCM-48	85.3	84.0	1.3 (1.5)
AlC48-40	92.2	80.8	11.4 (12.4)
AlC48-30	85.5	81.3	4.2 (4.9)
AlS48-20	84.6	78.9	5.7 (6.7)
AlC48-15	86.0	72.2	13.8 (16.0)
AlC41-40	43.5	43.0	0.5 (1.1)
AlC41-30	43.3	39.4	3.9 (9.0)
AlS41-20	42.9	39.7	3.2 (7.5)
AlC41-15	42.1	40.4	1.7 (4.0)

[a] Contraction of the unit cell parameter upon calcination (in angstroms) is followed (in brackets) by the contraction (in percent) with respect to the as-synthesized material.

As the aluminum content increases, the quality of the samples deteriorates, and the XRD peaks overlap and decrease in intensity (Figure 1). The fact that more aluminous gels are more difficult to crystallize is well-known in the synthesis of highly siliceous molecular sieves.[21] The unit cell parameters of as-synthesized and calcined samples and the contraction of the unit cell upon the removal of the surfactant are given in Table 2. The expansion in the unit cell with increasing aluminum content,[21,23] which is a rule in zeolite chemistry, is caused by the Al−O bond being longer (1.75 Å) than the Si−O bond (1.60 Å). Our results show that in mesoporous molecular sieves the situation is different: in aluminosilicate MCM-41[24] and MCM-48 the substitution of the silicon by aluminum leads to the *contraction* of the unit cell.

Thermal Analysis. The results of thermogravimetric (TG) and differential thermal analysis (DTA) of purely siliceous and aluminosilicate MCM-48 are shown in Figure 2. The TG curves consist of three distinct parts: the first corresponds to the loss of physisorbed water (ca. 10% weight loss) which nears completion at ca. 175 °C and is accompanied by maxima in the DTA and DTG curves (not shown). The first maximum, at ca. 80 °C, corresponds to water molecules adsorbed on the external surface of the solid, and the second, at ca. 150 °C, to water molecules occluded in the pores. The second part of the TG curve, at 175−350 °C, reflects the thermal removal of the template (ca. 40% weight loss). The third part, at 350−600 °C, is attributed to the desorption of the remaining template and/or water loss due to condensation of silanol groups to form siloxane bonds (ca. 15% weight loss). Weight loss is accompanied by an endothermic effect in the DTA curves (Figure 2).

Diffuse Reflectance Fourier Transform Infrared (DRIFT). All calcined samples give a sharp band at 3739 cm^{-1} arising from isolated Si−OH hydroxyl groups (Figure 3). In addition, sample AlC48-15 shows a broad band at ca. 3325 cm^{-1} attributed[25] to water and/or bonded silanol groups (Figure 2e). A number of bands are in evidence in the "skeletal region" (below 2500 cm^{-1}): the very weak band at ca. 1630 cm^{-1} (bending mode of H_2O), the broad band at 1061 cm^{-1} with a shoulder at 1220 cm^{-1}, and the bands at 810 and 451 cm^{-1} are all characteristic of SiO_2 and correspond to asymmetric and symmetric Si−O stretching and Si−O−Si bending, respectively.[26−29] The band at 571 cm^{-1} is assigned to bending vibrations of the surface $Si-O^-$ groups.[29] The absence of a band at 980 cm^{-1}, reported for crushed silica, silica gels, and zeolites containing a high concentration of defects,[29−31] indicates a high degree of polycondensation.

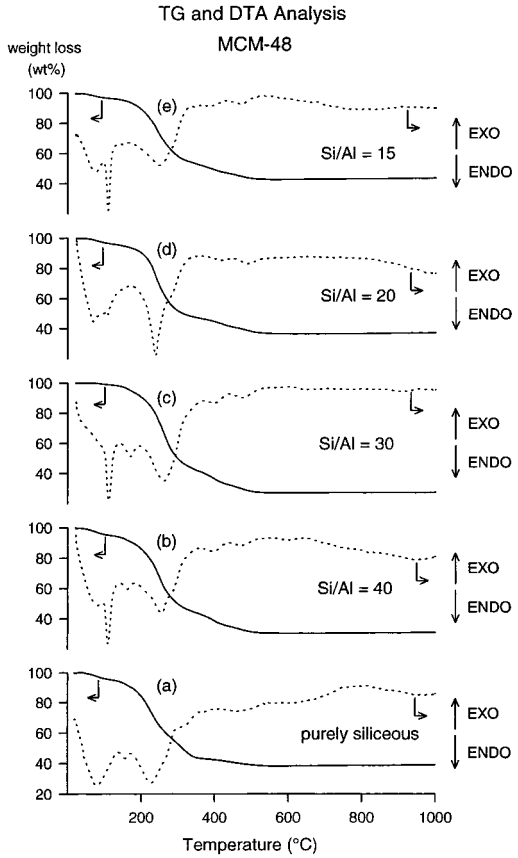

Figure 2. TG (solid lines) and DTA (dotted lines) plots for purely siliceous and aluminosilicate MCM-48. (a) Si−MCM-48, (b) AlC48-40, (c) AlC48-30, (d) AlS48-20, and (e) AlC48-15.

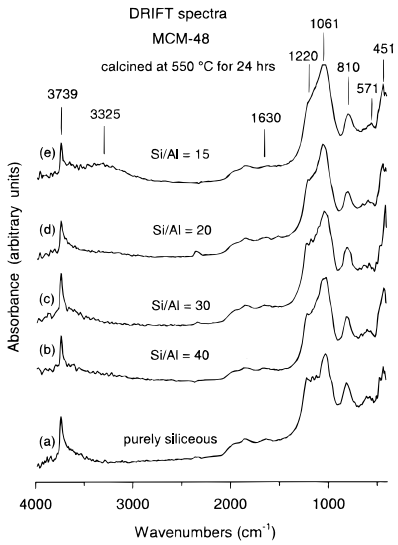

Figure 3. DRIFT spectra of purely siliceous and aluminosilicate MCM-48. (a) Si−MCM-48, (b) AlC48-40, (c) AlC48-30, (d) AlS48-20, and (e) AlC48-15. Samples were treated at 300 °C in 50 mL min^{-1} flow of nitrogen for 1 h, and the spectrum was measured at 300 °C against KBr reference.

^{29}Si MAS NMR. The ^{29}Si MAS NMR spectra of as-synthesized and calcined aluminosilicate MCM-48 prepared using aluminum chloride as the source of aluminum (Figure 4) contain three main features: the peak at ca. −110 ppm from the $Si(OSi)_4$ units and peaks at −106 and −102 ppm corresponding to $Si(OSi)_3(OH)$ and $Si(OSi)_2(OH)_2$ units, respectively.

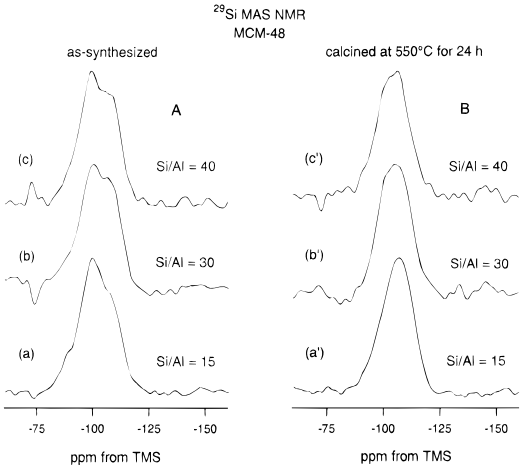

Figure 4. ^{29}Si MAS NMR spectra of as-synthesized and calcined aluminosilicate MCM-48 prepared using aluminum chloride as the source of aluminum and different Si/Al ratios. A: (curve a) as-synthesized AlC48-15, (curve b) AlC48-30, and (curve c) AlC48-40. B: (curve a′) calcined AlC48-15, (curve b′) AlC48-30, and (curve c′) AlC48-40.

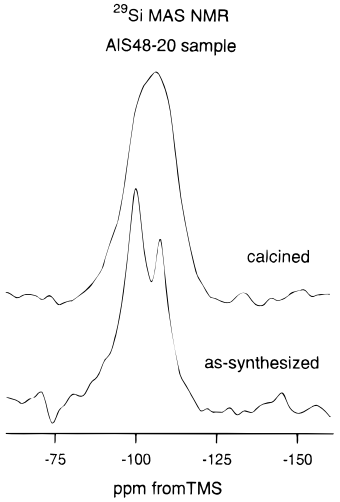

Figure 5. ^{29}Si MAS NMR spectra of as-synthesized and calcined aluminosilicate MCM-48 prepared using aluminum sulfate as the source of aluminum and Si/Al = 20.

Given the Si/Al ratios of the samples, it is possible that the resonances at −106 and −102 ppm contain contributions from Si(3Si, 1Al) sites, respectively.

Although the Si/Al ratios of the framework can be calculated directly by deconvoluting ^{29}Si NMR spectra,[32] the procedure is not sufficiently accurate for materials with Si/Al > 10. In addition, in our case the peak corresponding to the Si(nAl) units are poorly resolved and deconvolution is further complicated by the presence of the peak at ca. −102 ppm corresponding to $Si(OSi)_3OH$ (Q^3) units.[17] The presence of Si−OH groups is confirmed by DRIFT and ^{1}H−^{29}Si CP/MAS NMR (see below).

Increased aluminum content of the gel is followed by a decrease in the intensity of the Si(4Si) peak. A considerable decrease of peak intensity due to the overlap of Si(2Si,2Al) (Q^4) with $Si(OSi)_3OH$ (Q^3) units has been observed upon calcination. This could be interpreted in terms of a condensation of Si−OH groups, in agreement with the unit cell contraction observed by XRD.

Figure 5 shows the ^{29}Si MAS NMR spectra of sample AlS48-20 (Si/Al = 20) synthesized using aluminum sulfate. Only two well-resolved lines, at −108 and −100 ppm, are found in the spectrum of the as-synthesized sample, in good agreement with the ^{29}Si MAS NMR spectra of aluminosilicate MCM-41 synthesized with the same aluminum source.[21] Upon calcination, the line shape of the ^{29}Si MAS NMR spectra is similar to that for aluminosilicate MCM-48 prepared using aluminum chloride hexahydrate.

As with aluminosilicate MCM-41,[33] the ^{29}Si MAS NMR spectra of aluminosilicate MCM-48 are very broad, showing that the structure lacks precise repeats of T position (where T stands for the central atom in the SiO_4 or AlO_4 tetrahedron) at the second nearest neighbor (T−T) length scale and the presence of a wide range of T−O-T bond angles. Aluminum in MCM-48 is therefore in a highly disordered environment.

The intensity of the line at −100 ppm in the ^{1}H−^{29}Si CP/MAS spectra is markedly increased (Figure 6) in comparison with ^{29}Si MAS spectra, again indicating an appreciable contribution of the $Si(OSi)_3OH$ (Q^3) units to this line.

^{27}Al MAS NMR. ^{27}Al MAS NMR spectra of the as-synthesized aluminosilicate MCM-48 samples (Figure 7) contain peaks at 56 and 0 ppm assigned to 4- and 6-coordinate

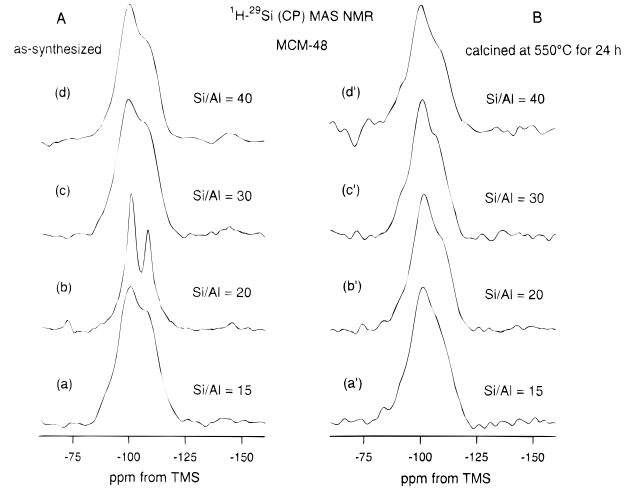

Figure 6. ^{1}H−^{29}Si CP/MAS NMR spectra of as-synthesized and calcined aluminosilicate MCM-48. A: (curve a) as-synthesized AlC48-15, (curve b) AlS48-20, (curve c) AlC48-30, and (curve d) AlC48-40. B: (curve a′) calcined AlC48-15, (curve b′) AlS48-20, (curve c′) AlC48-30, and (curve d′) AlC48-40.

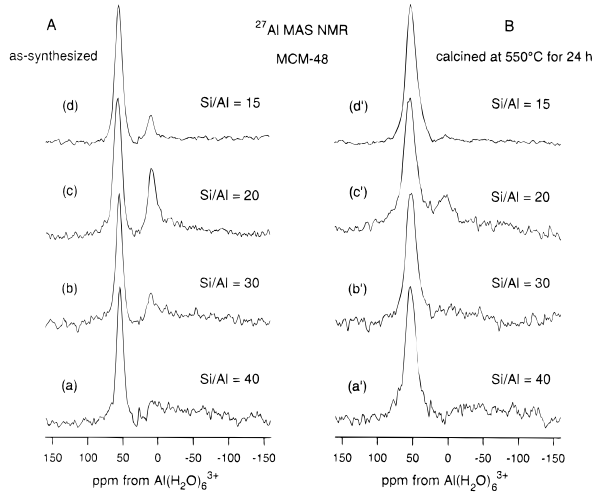

Figure 7. ^{27}Al MAS NMR spectra of as-synthesized and calcined aluminosilicate MCM-48 samples. A: (curve a) as-synthesized AlC48-40, (curve b) AlC48-30, (curve c) AlS48-20, and (curve d) AlC48-15. B: (curve a′) calcined AlC48-40, (curve b′) AlC48-30, (curve c′) AlS48-20, and (curve d) AlC48-15.

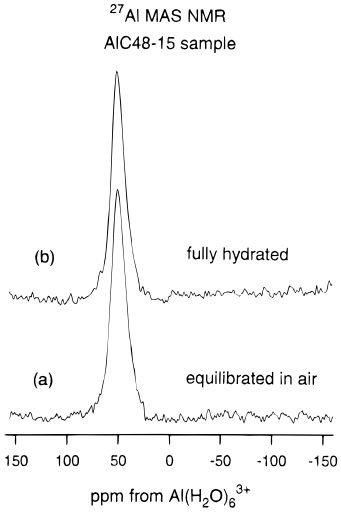

Figure 8. ^{27}Al MAS NMR spectra of calcined aluminosilicate AlC48-15 (curve a) equilibrated in air and (curve b) fully hydrated.

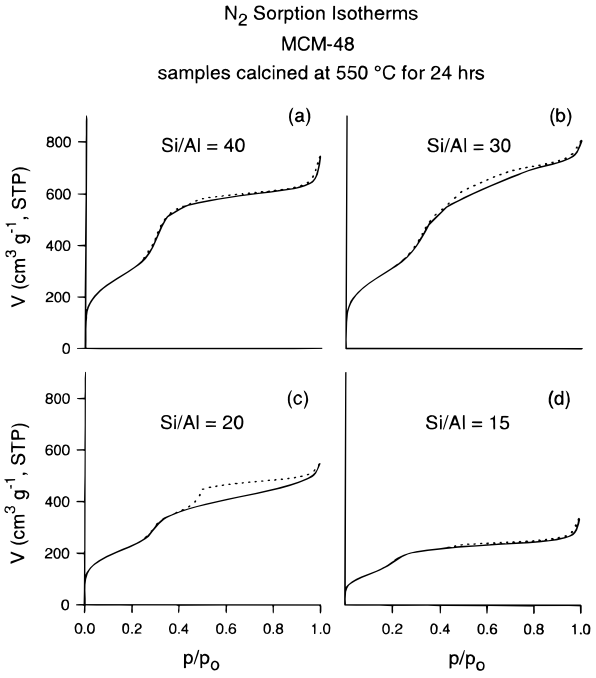

Figure 9. Adsorption (solid line) and desorption (dotted line) isotherms of nitrogen at 77 K on samples (a) AlC48-40, (b) AlC48-30, (c) AlS48-20, and (d) AlC48-15.

aluminum, respectively. As the Si/Al ratio decreases, the amount of 6-coordinate Al increases in as-synthesized aluminosilicate MCM-48 samples obtained using aluminum chloride hexahydrate. By contrast, the ^{27}Al MAS NMR spectrum of as-synthesized sample AlS48-20 shows a large peak at 0 ppm.

It is remarkable that no peak at 0 ppm, corresponding to 6-coordinate Al, is detected in calcined sample AlC48, indicating that all Al atoms are 4-coordinate[13] or the 6-coordinate aluminum is in such a highly distorted environment as to be undetectable by NMR under the conditions of the experiment.[34] The ^{27}Al MAS NMR spectrum of fully hydrated AlC48-15 was measured in order to establish whether 6-coordinate aluminum is still present upon calcination (Figure 8).[35] It is clear that, unlike in aluminum-containing MCM-41,[34,35] no dealumination of the MCM-48 network takes place. On the other hand, the spectrum of calcined sample AlS48-20 shows a peak at 0 ppm from 6-coordinate Al. These results show that, with aluminum

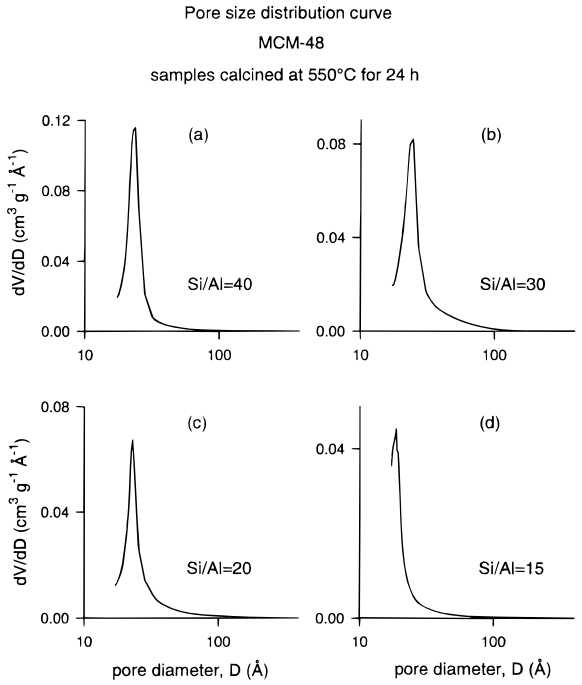

Figure 10. Pore size distribution curve calculated from the adsorption branch of the isotherm using the Barrett−Joyner−Halenda formula. (a) AlC48-40, (b) AlC48-30, (c) AlS48-20, and (d) AlC48-15.

TABLE 3: Cell Parameter and Pore Structure Parameters for the Products Calculated from the Adsorption Branch of the Nitrogen Sorption Isotherm Using the Barret−Joyner−Halenda Formula

sample	a (Å)	D_{BJH} (Å)	V_{BJH} (cm^3 g^{-1})	A_{BET} (m^2 g^{-1})
Si−MCM-48	84.0	22.6	1.09	1143
AlC48-40	80.8	23.6	0.90	1160
AlC48-30	81.3	23.3	1.03	1181
AlS48-20	78.9	22.8	0.67	846
AlC48-15	72.2	18.6	0.31	652
AlC41-40	43.0	27.4	1.17	1177
AlC41-30	39.4	27.7	1.32	1125
AlS41-20	39.7	27.4	0.96	1120
AlC41-15	40.4	24.8	0.94	999

sulfate as the source of Al, not all aluminum is incorporated in the silicate network.

The broadening of the ^{27}Al MAS NMR spectra upon removal of the surfactant is attributed to the highly distorted environment, resulting in large quadrupolar interactions and a wide range of T−O−T bond angles.[20,36]

N_2 Adsorption/Desorption Isotherms. The nitrogen adsorption/desorption isotherms of all samples of aluminosilicate MCM-48 and MCM-41 are similar irrespective of the source of aluminum used in the synthesis. Figure 9 shows the amount of nitrogen physisorbed at 77 K versus the relative pressure for aluminosilicate MCM-48. The isotherms are of Type IV, typical of mesoporous solids.[37] As the relative pressure increases ($p/p_o > 0.2$), the isotherms exhibit a sharp inflection characteristic of capillary condensation within the mesopores. This occurs at $p/p_o = 0.2$ and 0.4 for aluminosilicate MCM-48 (Figure 9) and MCM-41 (not shown), respectively. The sharpness of this step suggests a uniform size pore system. Adsorption at low relative pressures is caused by monolayer adsorption of N_2 on the walls of the mesopores and does not imply the presence of micropores, as verified by the *t*-plots (not shown).

Although the desorption branch of the isotherm is often used for the assessment of the distribution of mesopore sizes, a Type H3 hysteresis loop in unlikely to yield a reliable estimate of

pore size distribution, even for comparison purposes.[38] Accordingly, the pore size distribution (PSD) was obtained from the adsorption data by means of the Barrett−Joyner−Halenda (BJH) formula.[19] The comulative pore volume was calculated in the width range 15−400 Å. The mesopore diameter (D_{BJH}), comulative pore volume (V_{BJH}), and BET surface area (A_{BET}) are listed in Table 3.

The BJH plot (Figure 10) for the physisorption of N_2 on aluminosilicate MCM-48 gives a remarkably narrow pore size distribution with a pore size of ca. 22 Å (compared with 27 Å for aluminosilicate MCM-41). The sharp pore size distribution, with a ca. 6 Å width at half-height, shows that the mesopores are exceptionally uniform. This is supported by transmission electron microscopy.[17]

At high aluminum contents (Si/Al < 30), the BET surface area and mesopore volume of aluminosilicate MCM-48 fall sharply as the Si/Al ratio decreases. By contrast, in aluminosilicate MCM-41, with the Si/Al ratio as low as 15, the surface area and the mesopore volume are still very large (999 $m^2\ g^{-1}$ and 0.94 $cm^3\ g^{-1}$, see Table 3). It is clear that the incorporation of aluminum substantially lowers the quality of the aluminosilicate MCM-48, in agreement with the conclusions from the XRD.

Acknowledgment. We are grateful to the European Community for grants to M.D.A. and A.A.R. and to the Departamento de Química Orgánica, Universidad de Córdoba, for enabling us to perform the DRIFT and nitrogen adsorption measurements.

References and Notes

(1) Kresge, C. T.; Leonowicz, M. E.; Roth, W. J.; Vartuli, J. C.; Beck, J. S. *Nature* **1992**, *359*, 710.

(2) Beck, J. S.; Vartuli, J. C.; Roth, W. J.; Leonowicz, M. E.; Kresge, C. T.; Schmitt, K. D.; Chu, C. T. W.; Olson, D. H.; Sheppard, E. W.; McCullen, S. B.; Higgins, J. B.; Schlenker, J. L. *J. Am. Chem. Soc.* **1992**, *114*, 10834.

(3) Raman, N. K.; Anderson, M. T.; Brinker, C. J. *Chem. Mater.* **1996**, *8*, 1682.

(4) Sayari, A. *Chem. Mater.* **1996**, *8*, 1840.

(5) Zhao, X. S.; Lu, G. Q.; Millar, G. J. *Ind. Eng. Chem. Res.* **1996**, *35*, 2075.

(6) Sayari, A. In *Recent Advances and New Horizons in Zeolite Science and Technology;* Chon, H., Woo, S. I., Park, S. E., Eds.; Elsevier: Amsterdam, 1996; Chapter 1.

(7) Antonelli, D. M.; Ying, J. Y. *Curr. Opin Colloid Interface Sci.* **1996**, *1*, 523.

(8) Vartuli, J. C.; Schmitt, K. D.; Kresge, C. T.; Roth, W. J.; Leonowicz, M. E.; McCullen, S. B.; Hellring, S. D.; Beck, J. S.; Schlenker, J. L.; Olson, D. H.; Sheppard, E. W. *Chem. Mater.* **1994**, *6*, 2317.

(9) Schmidt, R.; Stöcker, M.; Akporiaye, D.; Tørstad, E. H.; Olsen, A. *Microporous Mater.* **1995**, *5*, 1.

(10) Zhao, D.; Goldfarb, D. *Stud. Surf. Sci. Catal.* **1995**, *97*, 181.

(11) Schmidt, R.; Stöcker, M.; Ellestad, O. H. *Stud. Surf. Sci. Catal.* **1995**, *97*, 149.

(12) Zhao, D.; Goldfarb, D. *J. Chem. Soc., Chem. Commun.* **1995**, 875.

(13) Schmidt, R.; Junggreen, H.; Stöcker, M. *J. Chem. Soc., Chem. Commun.* **1996**, 875.

(14) Kim, J. M.; Ryoo, R. *Bull. Korean Chem. Soc.* **1996**, *17*, 66.

(15) Zhang, W.; Pinnavaia, T. J. *Catal. Lett.* **1996**, *38*, 261.

(16) Morey, M.; Davidson, A.; Stucky, G. *Microporous Mater.* **1996**, *6*, 99.

(17) Romero, A. A.; Alba, M. D.; Zhou, W.; Klinowski, J. *J. Phys. Chem.* **1997,** *B101*, 5294.

(18) Sing, K. S. W.; Everett, D. H.; Haul, R. A. W.; Moscou, L.; Pierotti, R. A.; Rouquérol, J.; Siemieniewska, T. *Pure Appl. Chem.* **1985**, *57*, 603.

(19) Barrett, E. P.; Joyner, L. G.; Halenda, P. P. *J. Am. Chem. Soc.* **1951**, *73*, 373.

(20) Chen, C.-Y.; Li, H. X.; Davis, M. E. *Microporous Mater.* **1993**, *2*, 17.

(21) Reddy, K. M.; Song, C. *Catal. Lett.* **1996**, *36*, 103.

(22) Ryoo, R.; Kim, J. M. *J. Chem. Soc., Chem. Commun.* **1995**, 711.

(23) Borade, R. B.; Clearfield, A. *Catal. Lett.* **1995**, *31*, 267.

(24) Hamdan, H.; Endud, S.; He, H.; Muhid, M. N. M.; Klinowski, J. *J. Chem. Soc., Faraday Trans.* **1996**, *92*, 2311.

(25) Little, L. H. *Infrared Spectra of Adsorbed Species*; Academic Press: London, 1966.

(26) Laughlin, R. B.; Joannopoulos, J. D. *Phys. Rev. B* **1977**, *16*, 2942.

(27) Galeener, F. L.; Leadbetter, A. J.; Stringfellow, M. W. *Phys. Rev. B* **1983**, *27*, 1052.

(28) Bertoluzza, A.; Fagnano, C.; Morelli, M. A.; Gottardi, V.; Guglielmi, M. *J. Non-Cryst. Solids* **1982**, *48*, 117.

(29) Decottignies, M.; Phalippou, J.; Zarzycki, J. *J. Mater. Sci.* **1978**, *13*, 2605.

(30) Soda, R. *Bull. Chem. Soc. Jpn.* **1961**, *34*, 1491.

(31) Durán, A.; Serna, C.; Fornés, V.; Fernández-Navarro, J. M. *J. Non-Cryst. Solids* **1986**, *82*, 69.

(32) Engelhardt, G.; Michel, D. *High-Resolution Solid-State NMR of Silicates and Zeolites*; Wiley: Chichester, 1987.

(33) Luan, Z.; Cheng, C.-F.; Zhou, W.; Klinowski, J. *J. Phys. Chem.* **1995**, *99*, 1018.

(34) Schmidt, R.; Akporiaye, D.; Stöcker, M.; Ellestad, O. H. *J. Chem. Soc., Chem. Commun.* **1994**, 1493.

(35) Luan, Z.; Cheng, C.-F.; He, H.; Klinowski, J. *J. Phys. Chem.* **1995**, *99*, 10590.

(36) Oldfield, E.; Haase, J.; Schmitt, K. D.; Schramm, S. E. *Zeolites* **1994**, *14*, 101.

(37) Brunauer, S.; Deming, L. S.; Deming, W. S.; Teller, E. *J. Am. Chem. Soc.* **1940**, *62*, 1723.

(38) Gregg, S. J.; Sing, K. S. W. *Adsorption, Surface Area and Porosity*, 2nd ed; Academic Press: New York, 1982.